The influence of surface versus free-air decoupling on temperature trend patterns in the western United States

N. C. Pepin,[1] C. Daly,[2] and J. Lundquist[3]

Received 19 July 2010; revised 9 February 2011; accepted 18 February 2011; published 24 May 2011.

[1] We analyzed temperature trends from 460 GHCNv2 weather stations in the western United States for 1948–2006 to determine whether the extent of decoupling of surface temperatures from the free atmosphere influences past change. At each location we derived monthly indices representative of anticyclonicity using NCEP/NCAR 700 hPa reanalysis pressure fields. The number of anticyclonic days minus cyclonic days (A–C) is positively correlated with temperature anomalies at exposed convex sites and in the north of the domain where the free atmosphere controls temperature, anticyclonic months being warmer. In topographic concavities, and in the south of the domain where the influence of upper air ridges and troughs is muted, the relationship is much weaker. We use the gradient of the A–C index–temperature relationship to represent a coupling index, highest at exposed free-air locations. On a mean annual basis there are no strong relationships between temperature trend magnitude, elevation, topographic incision, or coupling index. However, in winter, warming is weaker at decoupled locations, especially when snow cover is present. Where snow is absent in winter, and in fall, the relationship is reversed. Circulation changes (increased cyclonicity) can explain the disparity in warming between decoupled and exposed locations in fall and to a certain extent in winter (increased anticyclonicity), although winter results are also regionally sensitive. Thus, future climate change may be different (amplified or muted dependent on season and/or surface characteristics) in locations prone to surface decoupling, compared with locations exposed to the free atmosphere. Understanding such processes will aid downscaling of future climate change.

Citation: Pepin, N. C., C. Daly, and J. Lundquist (2011), The influence of surface versus free-air decoupling on temperature trend patterns in the western United States, *J. Geophys. Res.*, *116*, D10109, doi:10.1029/2010JD014769.

1. Introduction

[2] Most simulations of future climate change are based primarily on models of large-scale free atmospheric behavior, and as a consequence it is difficult to downscale predictions of climate warming to the local scale [*Wilby and Wigley*, 1997], particularly in areas of complex relief. Local- and regional-scale processes, such as cold air drainage flow or the trapping of cold dense air masses by relief, effectively decouple the lower atmosphere from the regional signal, resulting in surface temperatures which can be markedly different from those expected from simple downward extrapolation of free-air temperature fields [*Sairouni et al.*, 2008; *Sheridan et al.*, 2010; *Daly et al.*, 2010]. Lower surface temperatures are commonly associated with the development of a temperature inversion in the lowest layers of the atmosphere [*Whiteman*, 1982; *Clements et al.*, 2003], which is often constrained by topography: valley bottom locations being under the inversion, while hilltops can protrude above [*Lundquist et al.*, 2008].

[3] Because of the variable temporal and spatial occurrence of this decoupling, spatial patterns of temperature are difficult to model in areas of complex relief, and understanding inversion formation and destruction is one of the most challenging meteorological forecast problems [*Smith et al.*, 1997; *Sheridan et al.*, 2010; *Gustavsson et al.*, 1998; *Pagès et al.*, 2008]. The issue is also central to the task of climate forecasting on a regional basis [*Giorgi and Francisco*, 2000; *Murphy*, 2000; *Mearns et al.*, 2001; *Stahl et al.*, 2006; *Daly et al.*, 2007]. Systematic surface temperature patterns can sometimes be discovered using a synoptic climatological approach [*Hay et al.*, 1992; *Yarnal*, 1993; *Conway and Jones*, 1998; *Crane and Hewitson*, 1998; *Wilby et al.*, 1999], since decoupling is strongly dependent on local cloud cover [*Kahl*, 1990] and wind conditions, which in turn are dependent on the upper level pressure pattern. The importance of upper level flow strength (usually 500–700 hPa) in controlling the extent of surface decoupling has long been recognized, with strong mechanical forcing from above often responsible for

[1]Department of Geography, University of Portsmouth, Portsmouth, UK.
[2]Department of Geosciences, Oregon State University, Corvallis, Oregon, USA.
[3]Department of Civil and Environmental Engineering, University of Washington, Seattle, Washington, USA.

0148-0227/11/2010JD014769

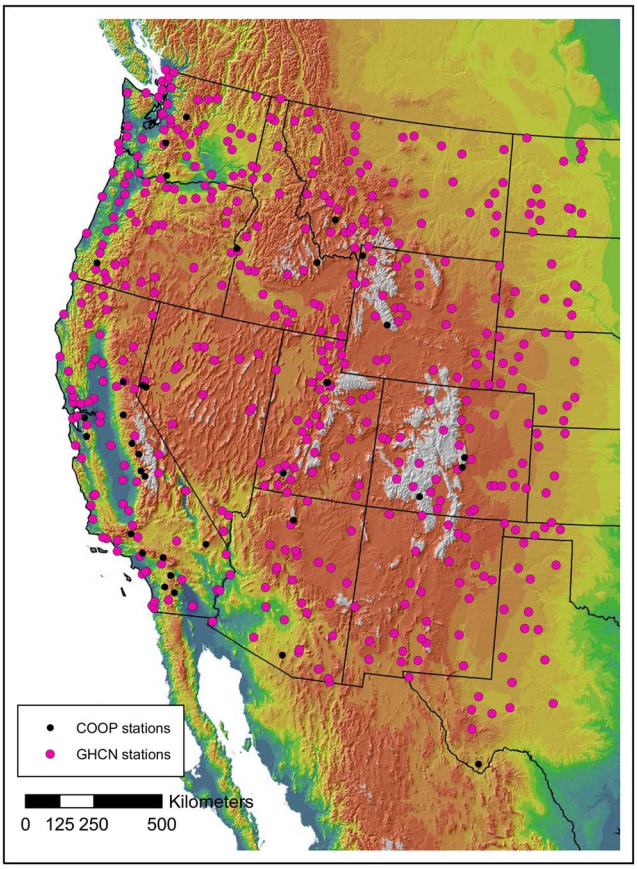

Figure 1. Location map of the western United States showing the distribution of the 460 GHCNv2 stations and 34 COOP stations.

inversion destruction and breakup [*Banta and Cotton*, 1981; *Banta*, 1986; *Maki and Harimaya*, 1988; *Clements et al.*, 2003; *Whiteman et al.*, 2004a]. Thus a broad generalization is that high-pressure conditions with atmospheric subsidence, limited cloud cover, and lack of wind, are the most conducive for low-level inversion formation [*Yoshino*, 1984; *Iijima and Shinoda*, 2000; *Kassomenos and Koletsis*, 2005], while during storms, the atmosphere tends to be well mixed [*Lundquist and Cayan*, 2007; *Barry*, 2008].

[4] In the context of climate change, *Daly et al.* [2010] demonstrated for the Oregon Cascades that monthly temperature anomalies at low-level valley locations show limited correlation with free atmospheric forcing (as defined by 700 hPa vorticity), whereas higher-elevation ridge top sites are well correlated. They go on to show that changes in circulation, as predicted by many GCMs [*Yin*, 2005; *Pinto et al.*, 2007; *Ulbrich*, 2009] would therefore have differential impacts at exposed ridge top and sheltered valley bottom sites. Despite the fact that similar differential sensitivity of climate stations to circulation has been shown in studies in many parts of the world [*Pepin*, 2001; *Pepin and Losleben*, 2002], there has been little work to examine whether this difference is still relevant when examining long-term temperature trends on a broad regional scale over the past 50–60 years. If cold air pooling was to become less frequent in a warmer world for example, local change would be amplified in such sensitive locations.

[5] This study sets out to assess whether locations prone to strong decoupling have seen enhanced or muted change in comparison with other locations over this extended time period, and whether more broadly, knowledge of atmospheric decoupling is relevant when considering climate change over decadal time scales. The relevance of such a study extends into many disciplines. Many sensitive species use cold air pools as refugia in times of climate uncertainty [*Millar and Westfall*, 2007], and absolute temperature minima and cold air pools are often important in an ecological context [e.g., *Tenow and Nilssen*, 1990; *Pypker et al.*, 2007]. Most of our current climate records are sited in relatively low level sites where most people live, particularly in mountainous regions. Cold pools both maintain and are strengthened by snow cover [*Whiteman et al.*, 2004b], can cause problems for transportation [*Bogren and Gustavsson*, 1991] and air pollution [*Allwine et al.*, 1992], and can act as a stabilizing influence against rapid free-air fluctuations, especially if saturated with low-level clouds. Most paleoclimate records are based on proxies taken from concavities in the landscape which are prone to decoupling, and therefore may not be representative of broader spatial scales [see *Stewart and Lister*, 2001; *Dobrowski*, 2011].

[6] We use the western United States as our study area, since the region has a relatively good coverage of climate data, is topographically complex, and the frequent dry and cloudless weather means that local decoupling is a major feature of the environment. After data and methods are outlined in section 2, section 3 explains how we quantify decoupling and model its variation in space. In section 4 we then examine the relationships between decoupling and past temperature trend magnitudes, before discussing wider implications in section 5 and concluding our findings in section 6.

2. Data and Methods

[7] We use monthly maximum and minimum temperature anomalies from 460 sites from the GHCNv2 climate data set [*Peterson and Vose*, 1997]. In the United States GHCN sites are a subset of the NWS COOP (National Weather Service Cooperative Observer Program) network, chosen for their relatively long and complete records. Our selection area runs from 100 to 125°W and from 29 to 50°N (Figure 1). Sites were only selected if they had at least 50 years of data within our chosen timeframe of 1948–2006 (59 years). Most had more than this. We extend beyond the traditional mountain ranges to include a range of sites with relatively simple topography, such as parts of the High Plains.

[8] The GHCNv2 data set has undergone extensive homogeneity adjustments to account for station moves, times of observations, changes in instrumentation, and other factors which would influence trends [*Peterson and Vose*, 1997]. Both adjusted and unadjusted versions are available, and we apply our analyses to both sets of data, so we can examine the effects of the adjustments. The sites are fairly evenly distributed across the study area. Figure 2a shows the elevation distribution of the GHCN stations. The stations are below the permanent snow line, but many develop a systematic winter snowpack. Most stations have a mean annual temperature

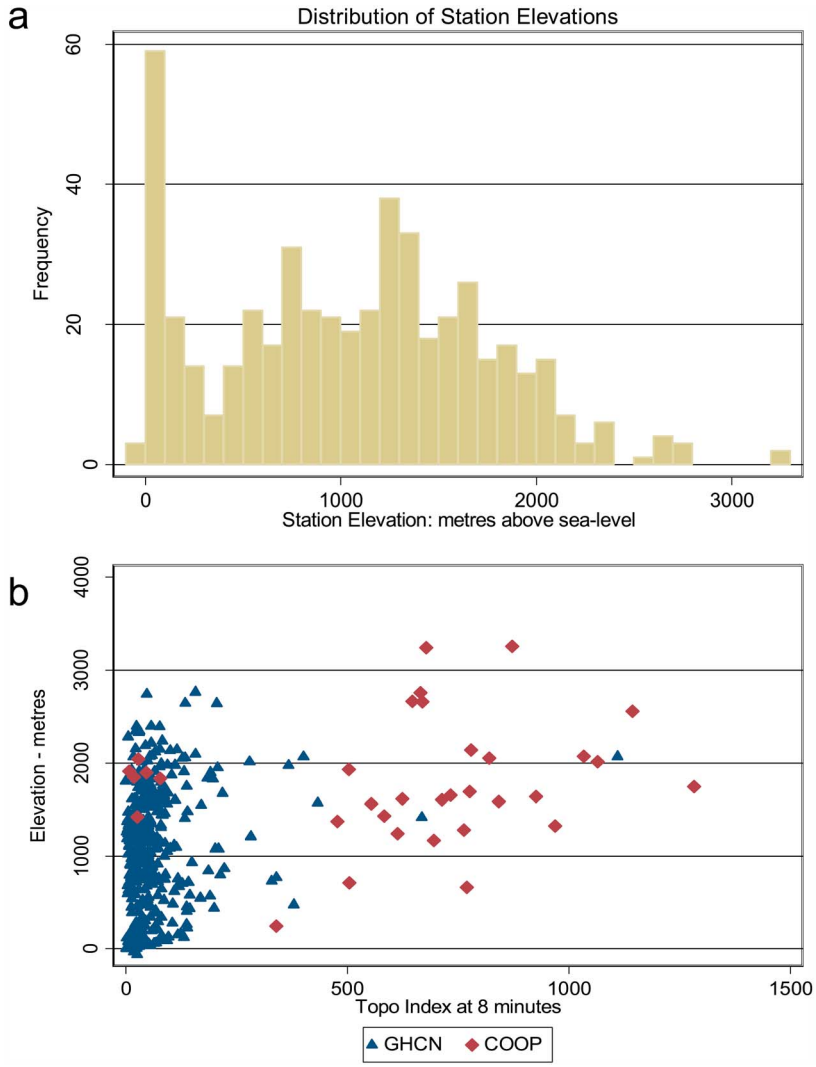

Figure 2. (a) Frequency distribution of station elevations (meters above sea level) and (b) relationship between station elevation and topographic index (see text for details).

between 5 and 15°C. The number of stations operating per year shows minimal variation during our time frame. Although more recent data sets, including the U.S Historical Climate Network (USHCNv2) [*Menne et al.*, 2009] are available, the coverage of stations is less extensive than in GHCNv2. It is also the case that many of the adjustments made in USHCNv2 are based on comparison with adjacent stations, which makes each station in theory less independent from its neighbors. It is possible that such adjustments could diminish local effects such as decoupling, but this requires further research.

[9] For each station we calculated a topographic index representative of whether the station was in a local concavity (valley bottom) or convexity (ridge top). This is because we hypothesize that decoupling from the free air will be more significant in concave localities because of the increased influence of the surface as opposed to the free atmosphere, and increased likelihood of cold air pooling. First we create a grid based on the pixels with the lowest elevations within a given search diameter (listed below). This minimum elevation grid was then averaged within the same diameter, and this averaged minimum elevation grid was subtracted from the original DEM to produce the topographic index. Further details are given by *Daly et al.* [2010]. The resultant index varies from zero (station at the lowest point in the local landscape) to a thousand meters or more (an isolated mountain peak). Flat areas will produce low numbers. Since the topographic index is scale dependent, we calculate this at three spatial scales; 2, 4 and 8 arc minutes (roughly equivalent to 2.6 km, 5.3 km and 10.5 km, respectively, at 45°N).

[10] Figure 2b shows the topographic index at the largest spatial scale for each of the GHCN stations plotted against elevation (blue triangles). The correlation between topographic index and elevation for GHCN stations is weak, meaning that elevation and topography (convexity/concavity) are largely independent. Indeed, many high-elevation stations are in mountain valleys. In particular, many of the long-term homogeneity-adjusted climate stations in the western United States are in areas with low topographic index, with very few mountain summit stations. Although this has been acknowledged in studies of global change [*Jones and Moberg*, 2003;

Table 1. Examples of Some of the 34 Supplementary COOP Stations Used in Topographical Analysis

Station	State	Latitude (°N)	Longitude (°W)	Elevation (m)	Topo Index (8 min)
Exposed summits					
Blowhard Mountain	UT	37.60	−112.87	3260	872
Mt. Hamilton	CA	37.34	−121.65	1282	763
Mt. Diablo	CA	37.88	−121.93	661	770
Kitt Peak	AZ	31.96	−111.60	2070	1144
Wolf Creek Pass	CO	37.48	−106.78	3243	678
Sexton Summit	WA	42.61	−123.37	1168	695
Known cold air pools					
Stanley	ID	44.22	−113.07	1911	7
Wisdom	MT	45.62	−112.55	1847	18
Seneca	OR	44.14	−117.03	1420	26
Truckee	CA	39.33	−119.81	1835	78
Jackson	WY	42.65	−109.24	1899	46
West Yellowstone	WY	44.66	−110.90	2042	28

Brohan et al., 2006], there have so far been few serious efforts to expand the mountain summit network or homogenize existing summit records, and planned long-term observational networks such as GCOS are deficient in this regard [*Bradley et al.*, 2004].

[11] To investigate the influence of topography on decoupling we supplement our terrain coverage by choosing 34 additional COOP stations in extremes of topographic exposure, to represent the range of topographic complexity within the western United States (diamonds in Figure 2b). Mountain summit stations were chosen by running our topographic index at all three scales on all potential COOP sites in the western United States and selecting those with the highest topographic indices and with the required number of years of record. At the other extreme we chose six well-known cold air pool locations in incised valleys, identified from papers outlining the locations of extreme minima recorded in the western United States [e.g., *King*, 2007]. Table 1 lists the six most exposed summits and all of the six cold pool locations. These additional stations mean that we can examine the relationships between decoupling and topography, but since the COOP stations are unadjusted in terms of homogeneity we do not use them in the trend analyses.

[12] Most of the GHCN and COOP stations also had snow depth data on a monthly basis (in mm), and we also use this in subsidiary analyses.

3. Quantification of Decoupling

3.1. Definition

[13] We define surface versus free-air decoupling as occurring when surface temperature anomalies at a site show no relationship with upper airflow patterns or synoptic climatology (Figure 3). Decoupling is not therefore synonymous with cold air pooling, but of a broader development of independent surface microclimates, and while cold air drainage is a strong cause of decoupling, it is not the only cause. In general anticyclonic conditions (high pressure and negative vorticity) are more likely to lead to local climate factors becoming more distinct. Lack of advection under high-pressure conditions maximizes local surface effects and temperature inversion formation, and thus the probability of surface inversions is

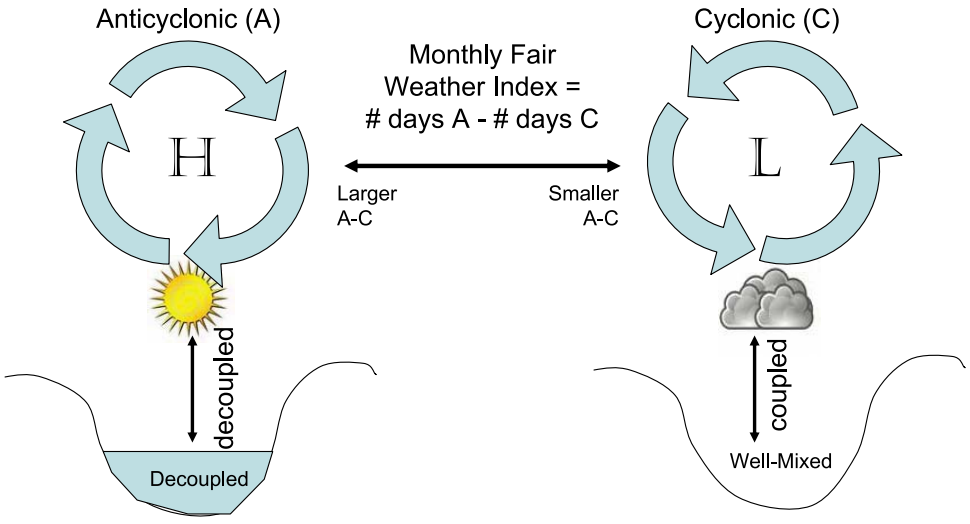

Figure 3. Schematic representation of the relationship between A–C index (degree of anticyclonicity) and its influence on surface versus free atmospheric decoupling. Temperatures at the ridge top site are strongly positively correlated with the A–C index, but those in the valley bottom may be decoupled.

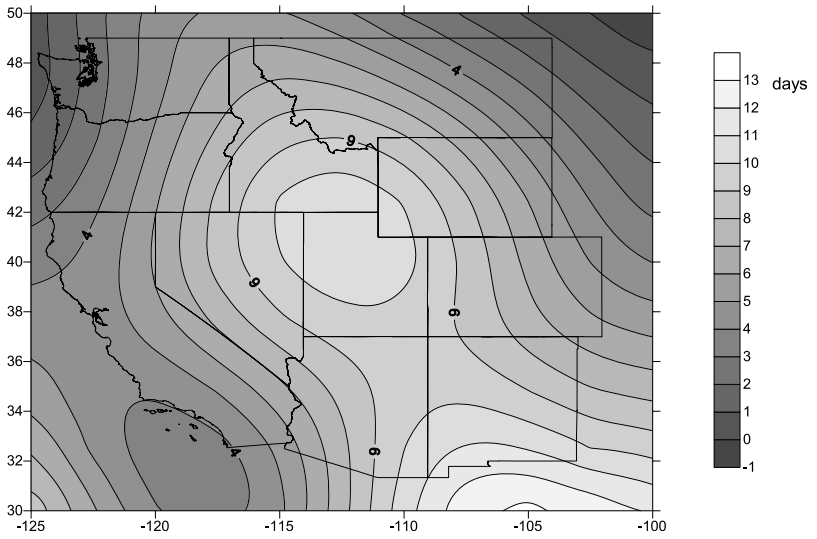

Figure 4. The mean monthly A–C index over the domain for 0000 UTC (1948–2006).

often inversely correlated with geopotential height contours [*Lundquist and Cayan*, 2007; *Lundquist et al.*, 2008]. This implies that surface temperatures (in decoupled locations) are less strongly controlled by the thermal structure of the free atmosphere when pressure is high.

[14] We develop an index representative of the extent of surface versus free atmospheric coupling based on the gradient of the relationship between surface temperature anomalies and free-air circulation. This is an extension of previous work by *Daly et al.* [2010] and is explained in detail below.

[15] Twice daily 700 hPa geopotential heights (0000 and 1200 UTC) were extracted from the NCEP/NCAR Reanalysis R1 [*Kistler et al.*, 2001] for 1948–2006 for the domain 90 to 135°W and 20 to 60°N. The pressure level data were at 2.5° resolution on a latitude/longitude grid. Geopotential heights were put into an objective algorithm based on *Lamb* [1972], *Jones et al.* [1993] and later used by *Losleben et al.* [2000] and *Daly et al.* [2010] to represent upper level flow strength and vorticity. Further details are given in these publications. The algorithm is centered on a particular grid point and allows a classification of each day's flow at that grid point as dominated by one of anticyclonic (A), cyclonic (C) or straight vorticity (zonal flow). After *Daly et al.* [2010], for each month we calculate the number of anticyclonic days and subtract the number of cyclonic days to create a "fair weather" index (A–C) at monthly resolution. Zonal flow days are ignored in this calculation.

[16] Since our temperature records are at varying locations across the western United States, we calculate the A–C index at each grid point across the domain. This was done by centering the grid used to calculate the index on the reanalysis grid point nearest to each GHCN or COOP station in turn. Figure 4 shows the mean index (1948–2006) for 0000 UTC. On average conditions tend to be more anticyclonic in the south and east of the domain than in the north and west, and there is a tendency for increased anticyclonicity over Utah associated with mean ridging in the upper level flow over the intermountain West. Similar patterns are seen for 1200 UTC. The index is on average higher in summer than in winter and spring, because an upper level ridge dominates the west in summer (maps not shown).

[17] We calculated the slope of the linear regression function fitted to the relationship between surface monthly temperature anomalies and the monthly A–C index (for the nearest grid point) at each station, over the entire time period. The slope coefficient (°C/d A–C change) represents the extent of coupling and is therefore a coupling index. This was calculated both for monthly average daily minimum temperatures (T_{min}) (compared with 1200 UTC A–C index, which ranged from 4:00 to 6:00 A.M. local standard time over our domain) and monthly average daily maximum temperatures (T_{max}) (compared with 0000 UTC A–C index, which ranged from 4:00 to 6:00 P.M. local standard time). A stronger gradient indicates more coupling between surface temperature anomalies and free-air circulation. Gradients are almost universally positive, but values range from around zero (effectively decoupled) to 0.3°C/d A–C change (high degree of coupling).

3.2. Spatial Patterns of (De)coupling

[18] Before we examine the effect of (de)coupling on long-term temperature trends, it is important to understand how it is spatially expressed. Figure 5 shows generalized maps of the coupling index for daytime maximum temperatures (Figure 5a) and nighttime minimum temperatures (Figure 5b). Broad spatial patterns of decoupling on an annual basis make intuitive sense. The T_{max} coupling index (Figure 5a) shows limited local variability and is synoptically controlled, reaching a maximum in the north of the region, particularly Montana, where upper level ridges and troughs compete for dominance. Stations along the West Coast, in particular in Oregon and California, show limited coupling; a semi-permanent surface inversion along the coast explains the decoupling in this area [*Dorman et al.*, 2000; *Filonczuk et al.*, 1995; *Leipper*, 1994]. Thus over the western coastal region where a persistent marine layer causes regional decoupling, and in the far south where synoptic variability is limited, the surface climate tends to be relatively decoupled from the A–C index. The more complex patterns of T_{min} coupling

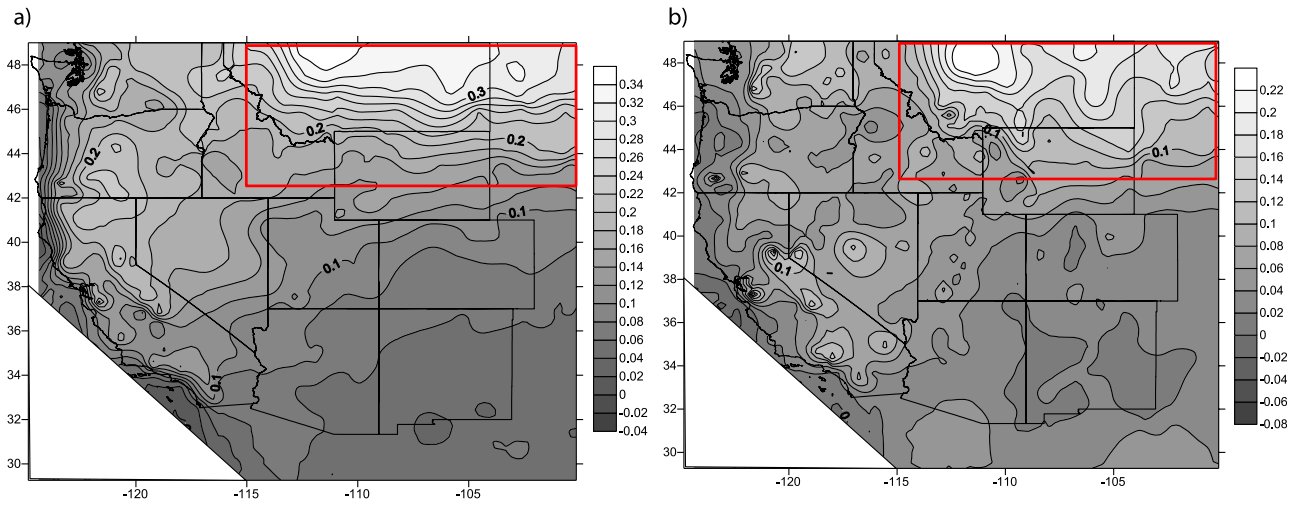

Figure 5. The spatial pattern of the coupling index (°C/d A–C change) for (a) daily maximum temperatures and (b) daily minimum temperatures. The highly coupled northeastern region is indicated by the solid box.

reflect a stronger influence of local topography on nocturnal temperatures compared to those of T_{max} (Figure 5b). This is consistent with studies of cold air pooling, which is much more prominent in T_{min} than T_{max} [*Whiteman*, 1982; *Clements et al.*, 2003; *Lundquist et al.*, 2008].

[19] We regressed the coupling indices against latitude, longitude, elevation and our topographic indices (at the three spatial scales). Table 2 lists significant correlations ($p < 0.05$) between spatial variables and the coupling indices. Results are shown for the year as a whole and for individual seasons. The total variance explained by all the topographic and locational variables is listed in the final column, and although not particularly high, clearly shows some success in modeling their spatial variance. The signs of the correlations of individual factors occasionally vary by season and time of day but are often consistent. Because our index is one of coupling, a positive correlation in Table 2 means that decoupling more commonly occurs with a decrease in that spatial variable. Thus in most seasons, decoupling more frequently occurs at lower latitudes (less distinct synoptic signal), further west in the domain, at lower elevations, and in relatively low lying areas (low topographic index). The signs of the relationships with topography are consistent during all seasons, and the scale of the topographic index used is relatively unimportant. Winter decoupling is dominated by larger-scale synoptic controls, and topography is not a significant predictor, whereas in spring and fall topography is relatively important. Decoupling usually decreases slightly at higher elevations, but was often omitted from regression models when run in stepwise mode (not shown). This may be a result of insufficient stations at the highest elevations, or because of the confounding effects of topographic position (see Figure 2).

[20] Figure 6 shows the relationship between our coupling index and the large-scale topographic index for T_{min} in the four seasons for all stations. Different scales are used on the *y* axis in different panels to increase clarity of presentation. Clearly topography is not the only control of decoupling, particularly in winter when the broad regional pattern (controlled by synoptics and shown in Figure 5b) is also a strong influence on our coupling index. Thus the winter graph shows a group of stations with low topographic index and high coupling (centered in Montana and parts of the northern tier of states). If we divide the domain into four quadrants using 115°W and 42.5°N as the dividing lines, the correlation between our coupling index and topographic

Table 2. Correlations ($p < 0.05$) Between Coupling Gradients and Topographical Variables Over the Western United States for Mean Annual Maximum and Minimum Temperatures, Seasonal Maximum Temperatures, and Seasonal Minimum Temperatures[a]

	Latitude	Longitude	Elevation	Topo8	Topo4	Topo2	R^2
T_{max} annual	**0.759**	**−0.136**	−0.091[b]				**0.591**
T_{min} annual	**0.575**	0.090[b]	0.100[b]	**0.217**	**0.202**	**0.199**	**0.498**
T_{max} DJF	**0.206**	**0.669**	**0.253**				**0.585**
T_{max} MAM	**0.307**	**0.237**	**0.255**	**0.158**	**0.141**	**0.136**	**0.244**
T_{max} JJA	**0.732**	**−0.137**	**−0.317**				**0.603**
T_{max} SON	**0.621**	**0.181**	**0.266**				**0.568**
T_{min} DJF	**0.500**	**0.463**	**0.157**				**0.664**
T_{min} MAM	**−0.167**	**0.346**	**0.386**	**0.476**	**0.463**	**0.436**	**0.401**
T_{min} JJA	**0.305**	**0.157**	**0.119**	**0.187**	**0.163**	**0.169**	**0.212**
T_{min} SON	**0.325**	**0.271**	**0.250**	**0.339**	**0.325**	**0.304**	**0.432**

[a]Total variance explained, R^2 (using all variables), is given in the eighth column. Significant correlations are marked in bold ($p < 0.01$). All R^2 values are significant at <0.01.
[b]Significant at $p = 0.05$ but not $p = 0.01$.

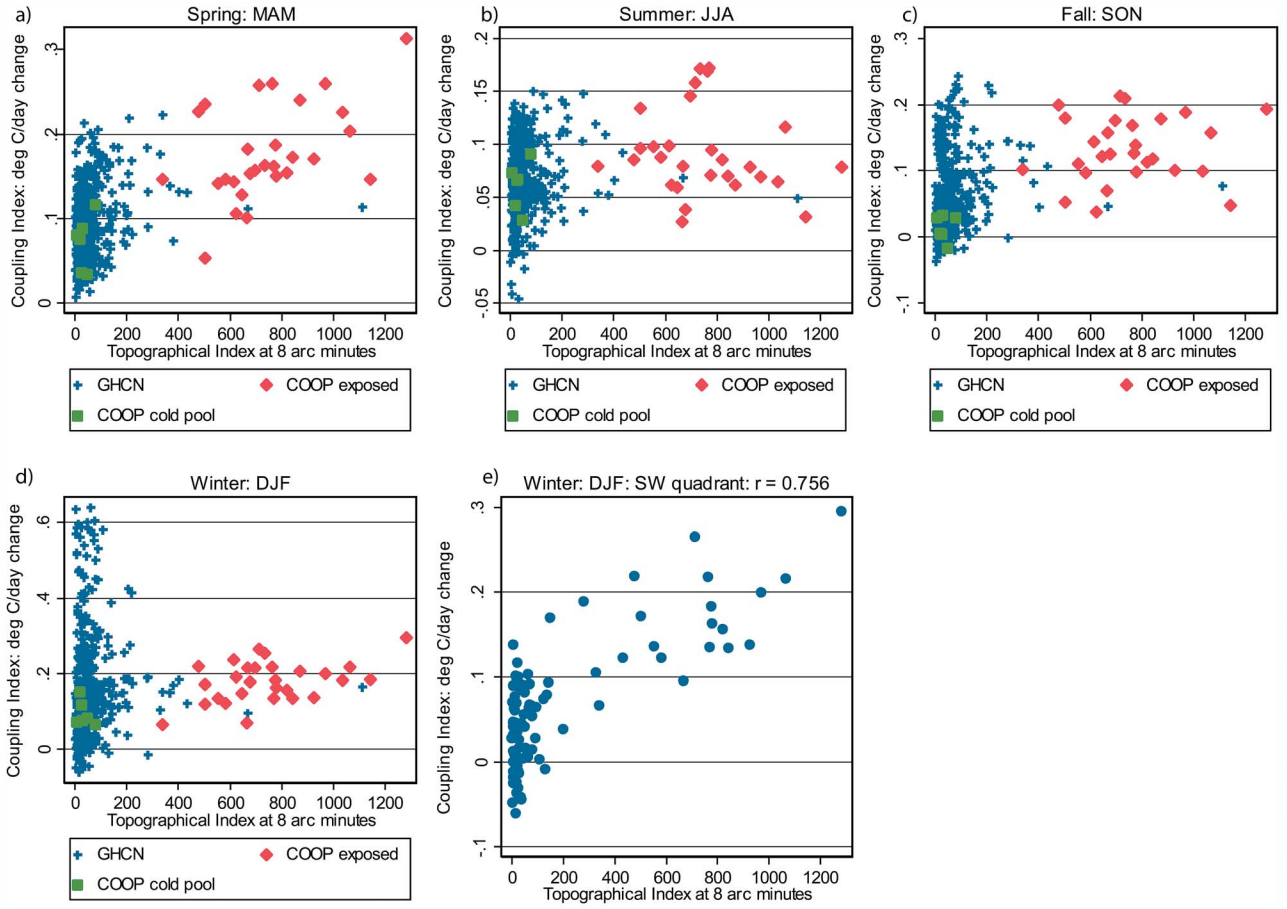

Figure 6. The relationship between the coupling index (minimum temperatures) and topographical index for (a) spring (MAM), (b) summer (JJA), (c) fall (SON), (d) winter (DJF), and (e) winter (DJF) in the SW quadrant (south of 42.5°N and west of 115°W) only.

index increases for sub areas. Collectively for the three quadrants outside the northeast, the correlation is 0.27 (n = 392) (graph not shown) and for the southwest quadrant 0.756 (n = 99) (Figure 6e), suggesting that outside the highly coupled northeastern region, topography is a stronger control of decoupling at night. In seasons other than winter the synoptic influence on decoupling is smaller and topographic influence stronger because the jet stream is usually much further north. Thus spring and autumn show stronger relationships between coupling and topography. Summer shows a weak pattern probably due to a combination of limited variation in circulation patterns during summer and shorter nights (which do not allow time for spatially extensive nocturnal driven cold pools to develop).

[21] In all the graphs the supplementary COOP stations (specifically chosen to cover the range of topography) dominate the variation along the topographic axis and show highly significant relationships ($p > 0.01$) between coupling and topography. In a broader sense, however, most of the exposed sites with high topographic index show high coupling (>0.05°C/d change), whereas sites with low topographic index show a much broader range of gradients. Thus incised topography appears a necessary but not sufficient requirement for strong decoupling. In summary, Figure 6 indentifies that there are competing regional- (synoptic) and local-scale (topographic) influences on decoupling, the latter being relatively more important at night. Thus in some further analyses we separate stations in the strongly coupled northeastern region (approximately Montana, eastern Idaho, northern Wyoming, and North Dakota) from the other stations.

4. Relationships Between Indices of Decoupling and Long-Term (1948–2006) Temperature Trends

4.1. Temperature Trends

[22] In our trend analysis we confine our results to the 464 GHCN stations since the supplementary COOP stations have not undergone homogeneity adjustment. The spatial patterns in western United States temperature trends (Figures 7a and 7b) are highly variable, as perhaps expected in such a topographically complex region. We defined the rate of warming by the gradient of an ordinary least squares regression line fitted to mean monthly temperature anomalies at a site over the period 1948–2006, and determined significance taking temporal autocorrelation into account [*Santer et al.*, 2000]. Many stations warmed during this period, with 204 (44.4%) stations showing significant ($p < 0.05$) T_{max} warming, rising to 307 (66.7%) for T_{min}. There are pockets of significant negative trends (32 stations for

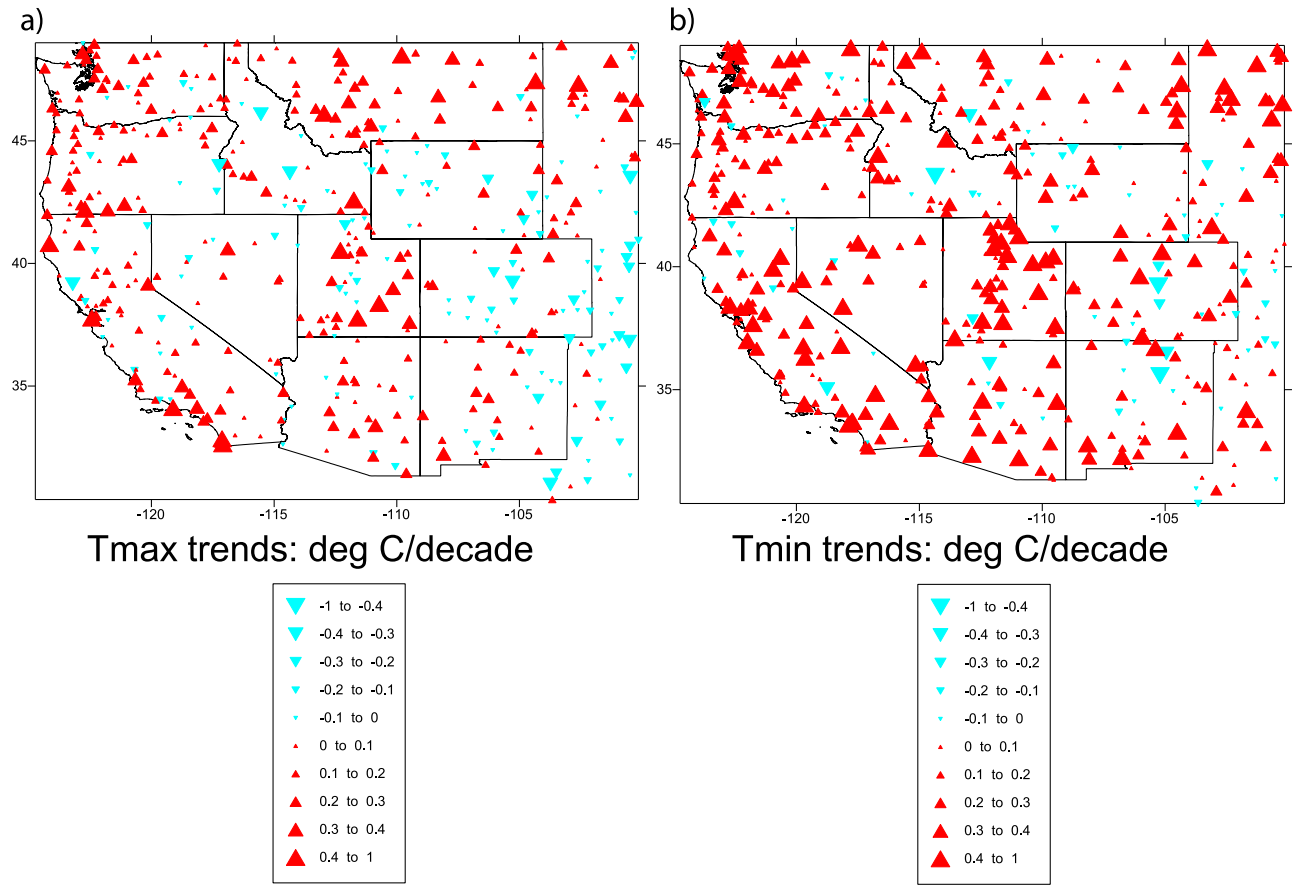

Figure 7. The spatial pattern of temperature trend magnitudes over the western United States (1948–2006) for (a) maximum temperatures and (b) minimum temperatures.

T_{min}). In general T_{min} trends are more positive (more warming) than those for T_{max} [*Karl et al.*, 1993]. In addition, the map of T_{min} trends (Figure 7b) shows more local-scale variability than the T_{max} map. Mean trend magnitudes are 0.16°C/decade and 0.21°C/decade for T_{max} and T_{min} temperatures, respectively (adjusted data), which agree broadly with studies in other regions of the globe [*Brohan et al.*, 2006; *Solomon et al.*, 2007].

[23] On an annual basis there are no strong significant relationships between elevation, topography and temperature trend magnitude (not shown). This is in contrast to some studies which claim enhanced warming at higher elevations either in the United States or elsewhere [*Diaz and Bradley*, 1997; *Chen et al.*, 2003; *Fyfe and Flato*, 1999; *Diaz and Eischeid*, 2007; *Giorgi et al.*, 1997; *Liu and Chen*, 2000; *Liu et al.*, 2009]. Some of these studies tended to use future model simulations rather than past climate records, while other studies have not replicated such claims [*Vuille et al.*, 2003; *Appenzeller et al.*, 2008; *You et al.*, 2008; *Pepin and Seidel*, 2005; *Pepin and Lundquist*, 2008].

4.2. Trends in Circulation (the A–C Index)

[24] We also calculated least squares linear trends in the A–C index at all grid points from 1948 to 2006, and in most cases the long-term trends were insignificant or very small (Figure 8). On an annual basis long-term trends were insignificant over the vast majority of the domain (not shown), but some seasonal trends were significant, although inconsistent [see *Abatzoglou and Redmond*, 2007]. In fall there has been a significant increase in cyclonicity over much of the region (Figure 8d), implying more frequent storms. The rate of increase ranges from around 0.5 days to over 1 d/decade. Winter has seen more frequent anticyclonicity in the north of the domain, but more frequent cyclonicity in the south, suggesting a more active southern storm track (Figure 8a), consistent with the shift in the Pacific Decadal Oscillation (PDO) over the time period examined [*Mantua et al.*, 1997]. In section 4.3 we examine whether these changes can account for spatial contrasts in warming rates.

4.3. The Relationship Between Temperature Trends and (De)coupling

[25] We expect a theoretical temperature trend at any given location to be a function of (1) the large-scale net radiation balance (i.e., increasing downward longwave radiation over the globe caused by increases in greenhouse gas emissions would be expected to result in positive trends), (2) changes in circulation patterns over the period examined (e.g., more or fewer clouds and/or cold winter storms), and (3) local land cover characteristics (e.g., changes in local shading or sky view factor due to changes such as vegetation cover). Here we focus on site-specific variations in temperature trends due to changes in circulation patterns over the period examined by assessing how temperatures at each site respond

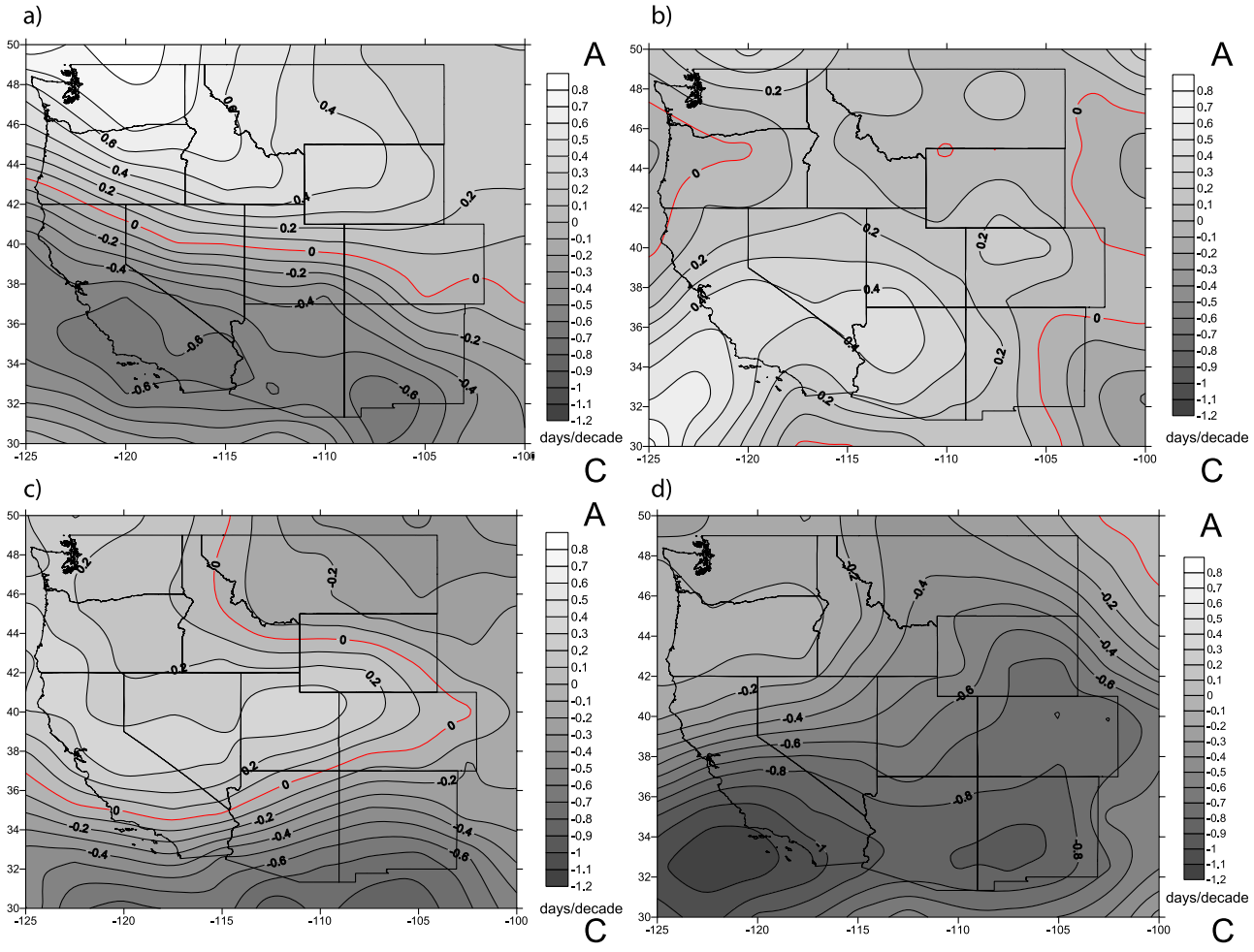

Figure 8. Long-term changes in circulation (A–C index) over the domain. The negative numbers (d/decade) mean an increase in the frequency of cyclonic conditions. (a) Winter (DJF), (b) spring (MAM), (c) summer (JJA), and (d) fall (SON).

to circulation changes (the coupling index) and how this in turn influences the temperature trends reported. Supplementary COOP stations are excluded from these analyses.

[26] The patterns of coupling, as represented by the coupling indices (Figure 5), show some spatial autocorrelation. So do the temperature trends, but to a lower extent (Figure 7). Because of this, conventional significance levels when assessing correlations between these variables are unrealistically low (often $p < 0.001$, even for correlations of 0.1–0.2), since in reality one station is not technically independent from those nearby [*Clifford et al.*, 1989; *Griffith*, 2005]. We do not quote significance levels in our discussion because of this issue, to avoid giving credence to "significant" relationships (e.g., $p < 0.001$) which nevertheless are somewhat superfluous. We measured autocorrelation using the Moran's I statistic, and using an approximation based on *Dale and Fortin* [2009] we were able to estimate new effective (reduced) sample sizes. These ranged from 172 to 394 for the analyses below (original $n = 460$). To be conservative we confine ourselves to a discussion of correlations higher than 0.3 in the following text (this would be equivalent to assuming an effective sample size of 31 for $p < 0.05$).

[27] Table 3 lists correlations between our coupling index (defined in section 3.1) and the magnitude of the annual and seasonal long-term temperature trends (1948–2006), for all stations based on unadjusted and adjusted GHCN data. On an annual basis (all stations) there is no strong relationship between the overall trend magnitude and the coupling index. On a seasonal basis, however, we find some higher correlations ($r > 0.3$). For both T_{max} and T_{min}, correlations between trend magnitude and coupling index are positive in winter (which showed a preference toward increased anticylonicity over the period over much of the domain (Figures 8a and 8b)), and for T_{min} the correlation is negative in fall (which showed increased cyclonicity over the period over much of the domain (Figure 8d)). Correlations in the 0.3–0.4 range mean that there is much scatter, and that (de)coupling is not the only factor influencing climate change. However, decoupled locations show a distinct tendency to have warmed less rapidly than coupled sites in winter (more frequent inversions corresponding to increased anticyclonicity), but warmed more rapidly in fall (less frequent inversions corresponding to increased cyclonicity). Spring and summer show limited correlation. Using adjusted or unadjusted GHCN data makes relatively little difference to the results.

Table 3. Annual and Seasonal Correlations Between the Coupling Index and the Rate of Temperature Change for GHCN Maximum and Minimum Temperatures[a]

	Annual	DJF	MAM	JJA	SON
T_{max} non-adj	0.205	0.256	0.169	−0.110	−0.235
T_{max} adj	0.188	0.375	0.195	−0.060	−0.217
T_{min} non-adj	0.015	0.248	0.082	−0.119	−0.350
T_{min} adj	0.040	0.320	0.0002	−0.081	−0.328

[a]"Adj" denotes GHCN adjusted data were used. Supplementary COOP stations are omitted.

[28] The above analysis includes all stations, even for areas (and seasons) where there has been no significant change in the A–C index. It is difficult, based on such analysis alone, to separate any circulation effect from other factors. For locations and in seasons where the A–C index has increased (more anticyclonicity) over the period of interest, we would expect greater than average temperature increases in highly coupled locations and smaller than average increases in decoupled locations. The opposite, however, would be true for locations and seasons where the A–C index has decreased. Using all stations, the fall relationship between coupling and temperature trend magnitude for T_{min} was negative (Figure 9a) ($r = -0.328$). This relationship strengthens slightly ($r = -0.352$) for the subsets of sites with significant ($p < 0.05$) circulation change. Thus coupled locations are experiencing preferential cooling associated with increased cyclonicity, with less change at the buffered decoupled locations. In winter, on the other hand, overall there is a positive relationship between coupling and temperature trend magnitude, with coupled sites warming more rapidly (Figure 9b) ($r = 0.375$). Again this pattern strengthens for stations with significant circulation change ($r = 0.475$) (Figure 9b). This is perhaps unsurprising since winter anticyclonicity has increased, and more frequent inversions would mean relatively subdued warming in decoupled locations.

[29] To separate regional and local forcings, we show separate analyses for the northern tier originally identified as well coupled in Figure 5b (all stations east of 115°W and north of 42.5°N (Figure 10a)) versus all other stations (Figure 10b). In the generally well-coupled northern tier, which is also snow covered in winter, there is a very strong positive relationship between coupling and the rate of temperature change for T_{max} ($r = 0.777$). Thus relatively decoupled sites are warming less rapidly and to some extent are buffered from the rapid warming otherwise seen in this coupled region. However, this relationship does not exist to the same extent outside this region (Figure 10b) and instead appears dependent on snow cover. For each site, mean winter (DJF) snow depth was extracted from the climate records. A mean snow depth of 20 mm and above was assumed to indicate persistent winter snowpack in most winters, and about half of the stations overall met this criterion (Figure 10c), mostly in the north of the domain, but also in the mountains of the Sierra Nevada, western Colorado, Nevada and the southwest (snowflake symbols). An examination of the relationship between decoupling and the rate of T_{max} change for snow covered and non snow covered locations separately (Figure 10b) for all stations outside the northern tier shows that the positive relationship between DJF coupling and warming remains for

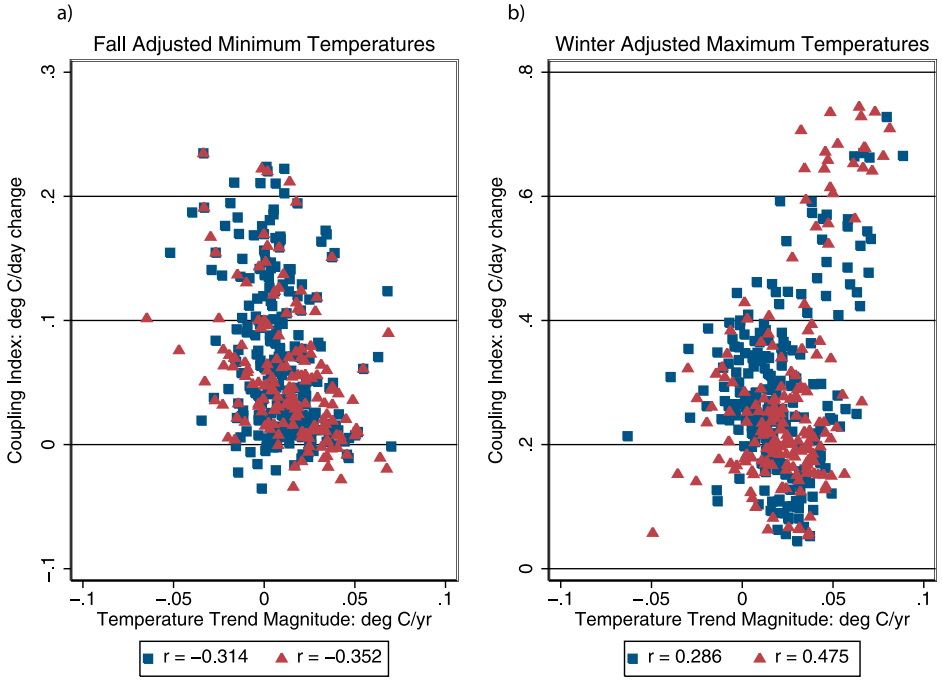

Figure 9. The relationship between the coupling index and seasonal temperature trends for (a) fall (SON) for stations with (triangles) and without (squares) significant circulation change and (b) winter (DJF) for stations with (triangles) and without (squares) significant circulation change. GHCN stations only are used in all analyses.

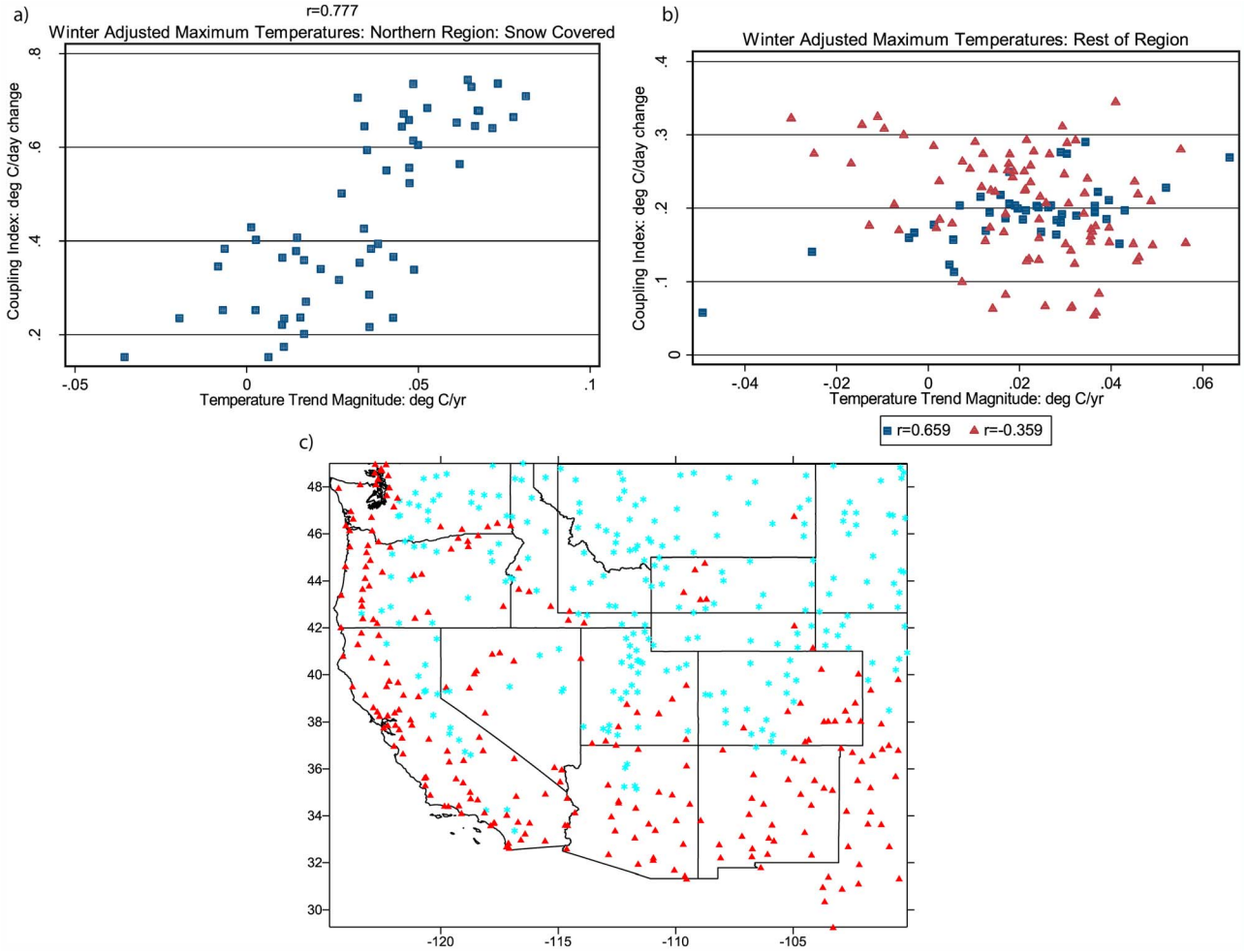

Figure 10. Winter (DJF) adjusted maximum temperature trends versus coupling index for (a) northern tier region east of 115°W and north of 42.5°N only (snow covered) and (b) all other stations including snowy (squares) and nonsnowy (triangles). (c) The location of snowy (snowflake symbol) and nonsnowy (upward triangle) stations in the western United States. A critical threshold of 20 mm was used to separate snowy and nonsnowy locations. The highly coupled northeastern region (used in Figure 10a) is delimited by the box covering parts of Idaho, Montana and Wyoming.

snow covered locations (r = 0.659), but reverses at non snow covered locations (r = −0.359).

[30] Thus the presence of snow cover in a decoupled location appears to reduce the warming rate compared to coupled locations. On the other hand, where snow cover is absent, the reverse relationship (albeit weaker) can be seen, and decoupled locations are actually warming faster. The above winter relationships also hold in a weaker form for T_{min} (not shown). These findings suggest that not all decoupled locations have acted in the same manner in the past, or will do so in the future. In the generally coupled northern tier, nearly all sites are snow covered in winter, so it is not possible to assess the influence of snow independent of larger-scale synoptic changes, but outside this region, where the synoptic control of coupling is weaker, and more local influences are critical, snow cover appears to have a strong effect.

Table 4. Multiple Regression Model Coefficients and Significance for All Variables With Dummy Variables Representing Presence/Absence of Circulation Change, Region, and Snow Cover[a]

	b_0	b_1	b_2	b_3	b_4	b_5	b_6	b_7
Variable	intercept	coupling	circulation change	region	snow	circulation interaction	region interaction	snow interaction
Coefficient	+0.131	−0.581	+0.106	−0.343	−0.231	−0.306	+1.046	+0.974
P value	0.000	0.000	0.007	0.000	0.000	0.016	0.000	0.000

[a]Interaction terms are also included. Terms b_o and b_1 provide the basic model. Terms b_2 to b_4 show the influence of that factor on the intercept of the general model, while terms b_5 to b_7 show the influence on the gradient (interaction terms). Overall r^2 is 0.362.

Table 5. Annual and Seasonal Correlations Between the Coupling Index and the Rate of Temperature Change for Maximum and Minimum Temperatures for the Regions Defined in Section 4.4[a]

	Region	Annual	DJF	MAM	JJA	SON
T_{max}	all data	0.188	0.375	0.195	−0.060	−0.217
T_{max}	region 1 (west of crest, <20 km from coast)	0.083	−0.252	0.211	0.150	0.050
T_{max}	region 2 (west of crest, >20 km from coast)	0.001	0.141	−0.034	0.152	−0.127
T_{max}	region 3 (east of crest)	0.254	0.498	0.280	−0.053	−0.137
T_{min}	all data	0.040	0.320	0.0002	−0.081	−0.328
T_{min}	region 1	−0.116	−0.004	−0.098	−0.125	−0.044
T_{min}	region 2	−0.185	−0.264	0.136	−0.058	−0.310
T_{min}	region 3	0.101	0.331	0.036	0.106	−0.309

[a]Adjusted data are used. COOP stations are omitted.

[31] Finally, to examine interaction between the effects of region, snow cover and circulation change in one unified model, we created a multiple regression model for winter T_{max} with dummy interaction terms. The base category was the region outside the northern tier with no snow and no significant circulation change. The coupling index was normalized meaning that b_0 represents the predicted temperature trend for average coupling for the base category (+0.13°C/decade). All other terms in the model were significant (Table 4) meaning that snow, region and circulation change all have significant independent effects on both the gradient and the intercept of the fitted model between coupling index and temperature trend magnitude. The coefficients b_0 and b_1 show that for the base category, coupling decreases the trend magnitude (weaker/stronger warming at coupled/decoupled sites). However, this effect is reversed in the northern Tier region (b_6) and by the presence of snow cover (b_7). Significant circulation change (b_5), on the other hand, strengthens the base category relationship (increased negative gradient between coupling and trend magnitude).

4.4. Regional Case Study: California and Oregon Coast

[32] The map of the coupling index for daily maximum temperature (Figure 5a) clearly shows that the western coastal region shows low values due to the extensive marine layer in this region. To investigate the unique behavior of west coast decoupling we separated these stations in California and Oregon from the rest of the region: region 1, all stations within 20 km of the coast (n = 36); region 2, all stations west of the Cascades and Sierra Nevada but further than 20 km from the coast (n = 44); and region 3, all other inland stations (n = 380).

[33] Table 5 lists the correlations between coupling index and rate of temperature change for these three regions. We used adjusted temperature trends, and supplementary COOP stations were again omitted. In many cases, especially in regions 1 and 2, spatial autocorrelation is weak and has little influence on significance. In region 3, however, we only discuss correlations above 0.3 as having any interest. Unsurprisingly, the relationships discussed in section 4.3 above are still present for region 3 (all inland stations) for winter and fall. However, they break down in the coastal region. There are no significant correlations at all between coupling index and warming rates in region 1, and nearly all the relationships disappear in region 2. This may be partly a result of the general lack of data. Because of the relatively small number of stations in the coastal regions, results were also sensitive to the exact delineation of the coastal zones (not shown). Clearly the coastal region behaves in a manner different than the vast majority of inland stations (region 3) and more research as to why this is the case is required.

5. Discussion and Implications

[34] We have found significant relationships between the extent of surface versus free-air decoupling and the rate of temperature change over the last 60 years in the western United States. On the scale of the western United States the relationships are seasonally and regionally dependent, and it is dangerous to make generalizations. On the annual scale there is no simple strong relationship between decoupling and warming rate over the last 60 years, although coupled locations dependent on circulation change appear to have been more consistent in their warming rates (mostly mountain summits). On the seasonal scale, in winter and spring, increased anticyclonicity (particularly in the north of the region) has tended to mean enhanced warming at coupled locations, with decoupled locations being buffered from this warming to some extent. In contrast, increased cyclonicity in fall has actually caused cooling at coupled locations, and there is a less consistent signal at decoupled locations. Because of varying changes in different seasons and regions, it is not easy to make general statements about the aggregated annual effects of such changes.

[35] So far observed changes in circulation have been rather small, and confined to certain seasons and/or subparts of the domain. This makes it difficult to see strong relationships between decoupling and temperature trends. However, if circulation changes were to become more significant in the 21st century, attendant spatial contrasts in temperature response may become much clearer. We can use our knowledge of the variable gradient of temperature response to circulation change (our coupling index) to quantify the extra spatial variance in warming rates which would accompany a widespread and systematic change in circulation over the western United States. Although climate models have problems simulating local-scale climate variability, many are now attempting to simulate long-term changes in circulation patterns [*Yin*, 2005; *Pinto et al.*, 2007]. Over the western United States some scenarios suggest a northward migration of the jet stream, and a general strengthening of the Pacific high. This would mean more anticyclonic days in the south of the region, and possibly further north (for a discussion see *Christensen et al.* [2007]). Although circulation change will not be the same everywhere, only a 3 day increase in the mean A–C index would be required to add an extra 1°C of variability in

climate response between the most decoupled and coupled sites on an annual basis (for maximum temperatures, based on the variation in response gradients in Figure 5a). The influence in individual seasons would be much more than this. These figures are independent from and additional to any broad warming due to greenhouse emissions which is forecast to range from 2.1 to 5.7°C over the western United States for the A1B scenario in the next century [*Solomon et al.*, 2007, Table 11.1].

[36] Because we have shown decoupled locations to behave differently from more exposed free-air sites in their response to long-term change, another issue of representativeness becomes important. Examination of the variability in temperature trends (as opposed to the mean magnitude) shows that variability has been enhanced in decoupled locations in comparison with coupled locations. Dividing the stations into two equal groups using the median coupling index (section 3.1) as the boundary, the variance in trend magnitude is 0.035°C/decade versus 0.025°C/decade for decoupled versus coupled locations, respectively, for T_{max} trends, and 0.057°C/decade versus 0.035°C/decade for T_{min} trends (both differences are significant at $p < 0.01$). Thus temperature trends are more variable at decoupled locations.

[37] This is relevant to the design of a long-term climate monitoring network in the western United States (and elsewhere). In making our decisions about which surface data sets to use for temperature trend investigation in this study, it became clear that both GHCNv2 and USHCNv2 suffer from a topographic bias toward valley locations with very few mountain top sites, and it was necessary to use supplementary COOP sites to examine the influence of topography (although we could not use them for trends). Most long-term climate stations are located in topographically low-lying areas, and as such are likely to be decoupled to a greater degree than most of the landscape. This might not be relevant when acquiring local trends, but is a problem when attempting to scale up site trends to obtain regional estimates of climate trends from surface data. Increased variance of trends at decoupled sites (partly a result of the variable relationships between trends and decoupling we illustrate in this paper) would make this issue worse. On the other hand, it is a problem for climate modelers since trend predictions based on downscaling regional changes could be missing important local detail, which is systematically different from free-air changes. This issue is relevant to palaeoclimatologists who use proxies predominantly found in decoupled locations, such as lake chironomids [*Lotter et al.*, 1997], diatoms [*Stoermer and Smol*, 2001], sediment cores [*Battarbee*, 2000] and glaciers [*Oerlemans*, 2001] to reconstruct past patterns of climate variability and change. Such proxies would overestimate past climate variability in a spatial sense. The issues therefore of enhanced variance and/or consistent differences in trend identification from decoupled versus coupled sites deserve further research.

[38] The extent to which snow cover appears to strengthen the influence of circulation pattern in winter is another area requiring further research. Outside the northern tier the effect of decoupling on warming rates appears dependent on snow cover. To understand why this is the case, we have to examine the physics of decoupling. Although the influence of cold air pooling in areas of incised topography is not the only contributor to explain the contrast between decoupled and coupled locations, it is a major component, especially outside the highly coupled northern region. In a classic cold pool location under sunny conditions (positive radiation balance), the presence of snow cover will prevent solar radiation from warming the surface and the low-level air (albedo effect), and this will encourage thermal inertia (i.e., stabilize the temperature regime). Sublimation from the snow surface may also increase humidity and encourage low-level fog formation, which would magnify this effect. During periods of negative energy balance, the insulation from snow cover minimizes upward heat flux from the ground beneath the snow [*Whiteman et al.*, 2004a], which allows the efficient loss of longwave radiation from the snow surface to dominate the air temperature regime, encouraging low surface minimum temperatures. Overall, therefore, it is much more likely that any inversion which forms in a snow covered decoupled location will persist, since inversions break up through radiative heating from below as well as from synoptically driven and dynamically induced mixing from above [*Whiteman*, 1982]. In our analyses, because the positive relationship between coupling and temperature trend magnitude is strongest for T_{max}, it is likely that the high albedo of snow plays an important role in reducing warming at decoupled locations.

[39] Although the presence of snow cover and negative energy balance in maintaining inversions (during both day and night) is well appreciated in meteorology [*Barr and Orgill*, 1989; *Neff and King*, 1989; *Whiteman et al.*, 1999, 2004b], so far it has not been known whether this is acting as a brake on possible daytime climate warming rates in locations where winter snow cover is persistent. Our analysis suggests this could be the case wherever snow cover is substantial, and the local climate is decoupled. One could argue that any snow stabilizing effect is also important at exposed sites, but the point is that this influence is reduced in comparison with decoupled locations because of the increased influence of the free atmosphere (wind) and the reduced influence of the surface itself [*Barry*, 2008].

[40] Current snow cover trends in the western United States are predominantly negative [*Mote et al.*, 2005]. If snow cover were to disappear at a decoupled location, then based on the opposing signs of the correlations in Figure 10b, local decoupling would no longer work to the station's benefit, and warming rates could be steeper than at exposed coupled locations. Taken logically this means that the warming in snowy decoupled locations may be delayed until a critical threshold is reached when the snow disappears. Then there could be a step change with warming accelerating as the stabilizing effect of the snow cover is no longer present. This could be important for local managers and any people concerned with protecting such landscapes in the western United States to appreciate. Many cold adapted flora and fauna inhabit cold pool locations because of the distinct microclimates [*Millar and Westfall*, 2007; *Tenow and Nilssen*, 1990; *Virtanen et al.*, 1998], and the implications for them could be profound, especially at their southern limits [*Lesica and McCune*, 2004].

[41] Finally, there are some interesting issues which emerge as a result of spatial scale. Most of our relationships were extremely weak during summer. The correlation between topographic index and decoupling, although still present, was much weaker during this season, and there were no relationships uncovered between decoupling and rates of

temperature change. During summer cold air drainage is transient and typically only occurs for a few hours each night. It is therefore likely to be on a small spatial scale (highly localized), and we suspect that this was not picked up by our more regional analysis. Certainly summer cold air pools can be meters wide [*Yoshino*, 1975], and the landscape complexity is typically fractal in nature. In the Oregon Cascades, *Daly et al.* [2010] found that topographic position at the 150 m scale was the best predictor of the strength of decoupling, and it is possible that smaller scales play a major role. In such circumstances the spatial scale of investigation is critical to the findings obtained. We suspect that our topographic indices are on too large a scale to capture summer decoupling. If we were to examine smaller spatial scales, slight inaccuracies in station position would become critical.

[42] Convection is an additional influence in the summertime climate which operates on a small scale, and it notoriously difficult to model against the landscape. Daily maximum temperatures in particular will be controlled by the development of convective clouds in the afternoon. This suggests that our methodology might not be so helpful in the tropical regions of the world where local-scale convection is a strong control of climate, and atmospheric circulation, as represented by upper air level flow, less so.

[43] In a recent global analysis [*Pepin and Lundquist*, 2008] it was shown that areas of incised topography showed increased variance in temperature trends in comparison with exposed ridge top and summit sites. Thus mountain summits could be seen as important markers above a sea of low-elevation noise. However, the extent to which this result was controlled by decoupling was unknown. The present study has suggested that there is increased variance in temperature trends at decoupled locations on the scale of the western United States. However, results are dependent on season and the spatial scale examined. The identification of the coastal region as one where our relationships break down in most seasons, exemplifies the dangers of assuming that the same relationships are applicable in all locations. It is possible that examination of the problem at the scale of the individual drainage basin or watershed within the western United States [e.g., *Daly et al.*, 2010] will uncover even more complexity, and practitioners would be well advised to understand this. There is no better substitute than local climate monitoring for understanding future changes at the subwatershed scale.

6. Conclusions and Summary

[44] An analysis of temperature trends over the western United States since 1948, with particular emphasis on how local patterns of surface versus free-air decoupling have mediated these trends, shows important results. Incised topography is strongly related to patterns of decoupling, especially at night, but there are also regional contrasts in the strength of decoupling related to synoptic circulation patterns.

[45] On the annual scale there are no simple relationships between decoupling and trend magnitudes. It is not true to say that decoupled locations have been warming more or less rapidly than exposed free-air sites. However, on a seasonal basis, there has been less winter warming at decoupled sites, especially in snow covered locations, and in fall the warming has been enhanced. These patterns correspond with increased anticyclonicity in winter and increased cyclonicity in fall over the majority of our domain, but the influence of snow appears independent of circulation changes.

[46] It is important to add a caveat, mostly relevant to the interpretation of our findings. In this analysis we have defined coupling as the response of surface temperatures to upper level flow vorticity. Although this response is depressed locally in cold air pooling locations in comparison with exposed sites, there are other more regional factors which can depress surface response, particularly on the continental interior side of mountain ranges and along coastlines. In the former case, low-level arctic air masses periodically form widespread inversions on the High Plains, and in the latter case, the surface marine layer on the west coast is a persistent regional-scale feature, especially in summer. Thus these regional variations in response mean that local-scale cold air pooling is not the only cause of decoupling. Further work is required to explain the influence of such additional factors on decoupling and hence on temperature trends.

[47] On the broad continental scale, our research demonstrates that the extent of surface decoupling has influenced the pattern of past observed temperature trends, and is therefore likely to be of importance in controlling future trend patterns. Thus it is all the more important to concentrate on improving our estimates of local-scale patterns of climate and climate change, since an understanding of the current-day spatial complexity of climate is essential to accurately downscale predictions of future climate trends.

[48] **Acknowledgments.** The research undertaken in this paper was partly financed by a Royal Society International Travel Grant reference 2009R1/TG090105. We thank the Northwest Alliance for Computational Science and Engineering at Oregon State University for providing office space and computer facilities. We thank Wayne Gibson for help with calculating synoptic indices and Joseph Smith for the provision of GHCN/COOP climate data. We thank the three anonymous reviewers for extremely helpful comments on earlier drafts of this paper.

References

Abatzoglou, J. T., and K. T. Redmond (2007), Asymmetry between trends in spring and autumn temperature and circulation regimes over western North America, *Geophys. Res. Lett.*, *34*, L18808, doi:10.1029/2007GL030891.

Allwine, K. J., B. Lamb, and R. Eskridge (1992), Wintertime dispersion in a mountainous basin at Roanoke, Virginia: Tracer study, *J. Appl. Meteorol.*, *31*, 1295–1311, doi:10.1175/1520-0450(1992)031<1295:WDIAMB>2.0.CO;2.

Appenzeller, C., M. Begert, E. Zenklusen, and S. C. Scherrer (2008), Monitoring climate at the highest permanently manned meteorological station in Europe, *Sci. Total Environ.*, *391*, 262–268, doi:10.1016/j.scitotenv.2007.10.005.

Banta, R. M. (1986), Daytime boundary layer evolution over mountainous terrain. Part II: Numerical studies of upslope flow duration, *Mon. Weather Rev.*, *114*, 1112–1130, doi:10.1175/1520-0493(1986)114<1112:DBLEOM>2.0.CO;2.

Banta, R., and W. R. Cotton (1981), An analysis of the structure of local wind systems in a broad mountain basin, *J. Appl. Meteorol.*, *20*, 1255–1266, doi:10.1175/1520-0450(1981)020<1255:AAOTSO>2.0.CO;2.

Barr, S., and M. M. Orgill (1989), Influence of external meteorology on nocturnal valley drainage winds, *J. Appl. Meteorol.*, *28*, 497–517, doi:10.1175/1520-0450(1989)028<0497:IOEMON>2.0.CO;2.

Barry, R. G. (2008), *Mountain Weather and Climate*, 3rd ed., Routledge, London.

Battarbee, R. W. (2000), Paleolimnological approaches to climate change, with special regard to the biological record, *Quat. Sci. Rev.*, *19*(1–5), 107–124.

Bogren, J., and T. Gustavsson (1991), Nocturnal air and road surface temperature variations in complex terrain, *Int. J. Climatol.*, *11*(4), 443–455, doi:10.1002/joc.3370110408.

Bradley, R. S., F. D. Keimig, and H. F. Diaz (2004), Projected temperature changes along the American Cordillera and the planned GCOS network, *Geophys. Res. Lett.*, *31*, L16210, doi:10.1029/2004GL020229.

Brohan, P., J. J. Kennedy, I. Harris, S. F. B. Tett, and P. D. Jones (2006), Uncertainty estimates in regional and global observed temperature changes: A new data set from 1850, *J. Geophys. Res.*, *111*, D12106, doi:10.1029/2005JD006548.

Chen, B., W. C. Chao, and X. Liu (2003), Enhanced climatic warming in the Tibetan plateau due to doubling CO_2: A model study, *Clim. Dyn.*, *20*, 401–413.

Christensen, J. H., et al. (2007), Regional climate projections, in *Climate Change 2007: The Physical Science Basis—Contribution of Working Group I to the Fourth Assessment Report of the Intergovernmental Panel on Climate Change*, edited by S. Solomon et al., chap. 11, pp. 847–940, Cambridge Univ. Press, Cambridge, U. K.

Clements, C. B., C. D. Whiteman, and J. D. Horel (2003), Cold air pool structure and evolution in a mountain basin: Peter Sinks, Utah, *J. Appl. Meteorol.*, *42*, 752–768, doi:10.1175/1520-0450(2003)042<0752:CSAEIA>2.0.CO;2.

Clifford, P., S. Richardson, and D. Hémon (1989), Assessing the significance of correlation between two spatial processes, *Biometrics*, *45*, 123–134, doi:10.2307/2532039.

Conway, D., and P. D. Jones (1998), The use of weather types and airflow indices for GCM downscaling, *J. Hydrol.*, *212–213*, 348–361, doi:10.1016/S0022-1694(98)00216-9.

Crane, R. G., and B. C. Hewitson (1998), Doubled CO_2 precipitation changes for the Susquehanna Basin: Down-scaling from the Genesis general circulation model, *Int. J. Climatol.*, *18*(1), 65–76, doi:10.1002/(SICI)1097-0088(199801)18:1<65::AID-JOC222>3.0.CO;2-9.

Dale, M. R. T., and M. J. Fortin (2009), Spatial autocorrelation and statistical tests: Some solutions, *J. Agric. Biol. Environ. Stat.*, *14*(2), 188–206, doi:10.1198/jabes.2009.0012.

Daly, C., J. W. Smith, J. I. Smith, and R. B. McKane (2007), High-resolution spatial modeling of daily weather elements for a catchment in the Oregon Cascade Mountains, United States, *J. Appl. Meteorol. Climatol.*, *46*, 1565–1586, doi:10.1175/JAM2548.1.

Daly, C., D. R. Conklin, and M. H. Unsworth (2010), Local atmospheric decoupling in complex topography alters climate change impacts, *Int. J. Climatol.*, *30*, 1857–1864.

Diaz, H. F., and R. S. Bradley (1997), Temperature variations during the last century at high elevation sites, *Clim. Change*, *36*, 253–279, doi:10.1023/A:1005335731187.

Diaz, H. F., and J. K. Eischeid (2007), Disappearing "alpine tundra" Koppen climatic type in the western United States, *Geophys. Res. Lett.*, *34*, L18707, doi:10.1029/2007GL031253.

Dobrowski, S. Z. (2011), A climatic basis for microrefugia: The influence of terrain on climate, *Global Change Biol.*, *17*(2), 1022–1035, doi:10.1111/j.1365-2486.2010.02263.x.

Dorman, C. E., T. Holt, D. P. Rogers, and K. Edwards (2000), Large-scale structure of the June–July 1996 marine boundary layer along California and Oregon, *Mon. Weather Rev.*, *128*, 1632–1652, doi:10.1175/1520-0493(2000)128<1632:LSSOTJ>2.0.CO;2.

Filonczuk, M. K., D. R. Cayan, and L. G. Riddle (1995), *Variability of Marine Fog Along the California Coast*, *SIO Ref.*, vol. 95–2, 102 pp., Scripps Inst. of Oceanogr., Univ. of Calif., San Diego, La Jolla.

Fyfe, J. C., and G. M. Flato (1999), Enhanced climate change and its detection over the Rocky Mountains, *J. Clim.*, *12*, 230–243, doi:10.1175/1520-0442-12.1.230.

Giorgi, F., and R. Francisco (2000), Evaluating uncertainties in the prediction of regional climate change, *Geophys. Res. Lett.*, *27*, 1295–1298, doi:10.1029/1999GL011016.

Giorgi, F., J. W. Hurrell, M. R. Marinucci, and M. Beniston (1997), Elevation dependency of the surface climate signal: A model study, *J. Clim.*, *10*, 288–296, doi:10.1175/1520-0442(1997)010<0288:EDOTSC>2.0.CO;2.

Griffith, D. A. (2005), Effective geographic sample size in the presence of spatial autocorrelation, *Ann. Assoc. Am. Geogr.*, *95*(4), 740–760, doi:10.1111/j.1467-8306.2005.00484.x.

Gustavsson, T., M. Karlsson, J. Bogren, and S. Lindqvist (1998), Development of temperature patterns during clear nights, *J. Appl. Meteorol.*, *37*, 559–571, doi:10.1175/1520-0450(1998)037<0559:DOTPDC>2.0.CO;2.

Hay, L. E., G. J. McCabe Jr., D. M. Wolock, and M. A. Ayers (1992), Use of weather types to disaggregate general circulation model predictions, *J. Geophys. Res.*, *97*(D3), 2781–2790.

Iijima, Y., and M. Shinoda (2000), Seasonal changes in the cold-air pool formation in a subalpine hollow, central Japan, *Int. J. Climatol.*, *20*, 1471–1483, doi:10.1002/1097-0088(200010)20:12<1471::AID-JOC554>3.0.CO;2-6.

Jones, P. D., and A. Moberg (2003), Hemispheric and large-scale surface air temperature variations: An extensive revision and update to 2001, *J. Clim.*, *16*, 206–223, doi:10.1175/1520-0442(2003)016<0206:HALSSA>2.0.CO;2.

Jones, P. D., M. Hulme, and K. R. Briffa (1993), A comparison of Lamb circulation types with an objective classification scheme, *Int. J. Climatol.*, *13*, 655–663, doi:10.1002/joc.3370130606.

Kahl, J. D. (1990), Characteristics of the low-level temperature inversion along the Alaskan Arctic coast, *Int. J. Climatol.*, *10*(5), 537–548, doi:10.1002/joc.3370100509.

Karl, T. R., P. D. Jones, R. W. Knight, G. Kukla, N. Plummer, V. Razavayev, K. P. Gallo, J. Linseay, R. J. Charlson, and T. C. Peterson (1993), Asymmetric trends of daily maximum and minimum temperature, *Bull. Am. Meteorol. Soc.*, *74*, 1007–1023, doi:10.1175/1520-0477(1993)074<1007:ANPORG>2.0.CO;2.

Kassomenos, P. A., and J. G. Koletsis (2005), Seasonal variation of the temperature inversions over Athens, Greece, *Int. J. Climatol.*, *25*(12), 1651–1663, doi:10.1002/joc.1188.

King, G. (2007), The hottest and coldest places in the conterminous United States, *Yearb. Assoc. Pac. Coast Geogr.*, *69*, 101–114, doi:10.1353/pcg.2007.0008.

Kistler, R., et al. (2001), The NCEP/NCAR 50-year reanalysis, *Bull. Am. Meteorol. Soc.*, *82*, 247–267, doi:10.1175/1520-0477(2001)082<0247:TNNYRM>2.3.CO;2.

Lamb, H. H. (1972), *British Isles Weather Types and a Register of Daily Sequence of Circulation Patterns, 1861–1971*, *Geophys. Mem.*, vol. 116, 85 pp., Her Majesty's Stn. Off., London.

Leipper, D. F. (1994), Fog on the United States West Coast: A review, *Bull. Am. Meteorol. Soc.*, *75*, 229–240, doi:10.1175/1520-0477(1994)075<0229:FOTUWC>2.0.CO;2.

Lesica, P., and B. McCune (2004), Decline of arctic-alpine plants at the southern margin of their range following a decade of climatic warming, *J. Veg. Sci.*, *15*, 679–690, doi:10.1111/j.1654-1103.2004.tb02310.x.

Liu, X. D., and B. D. Chen (2000), Climatic warming in the Tibetan plateau during recent decades, *Int. J. Climatol.*, *20*, 1729–1742, doi:10.1002/1097-0088(20001130)20:14<1729::AID-JOC556>3.0.CO;2-Y.

Liu, X. D., Z. Cheng, L. Yan, and Z.-Y. Yin (2009), Elevation dependency of recent and future minimum surface air temperature trends in the Tibetan Plateau and its surroundings, *Global Planet. Change*, *68*, 164–174, doi:10.1016/j.gloplacha.2009.03.017.

Losleben, M. L., N. C. Pepin, and S. Pedrick (2000), Relationships of precipitation chemistry, atmospheric circulation and elevation at two sites on the Colorado Front Range, *Atmos. Environ.*, *34*, 1723–1737, doi:10.1016/S1352-2310(99)00431-8.

Lotter, A. F., H. J. B. Birks, W. Hofmann, and A. Marchetto (1997), Modern diatom, cladocera, chironomid, and chrysophyte cyst assemblages as quantitative indicators for the reconstruction of past environmental conditions in the Alps. I. Climate, *J. Paleolimnol.*, *18*(4), 395–420, doi:10.1023/A:1007982008956.

Lundquist, J., and D. Cayan (2007), Surface temperature patterns in complex terrain: Daily variations and long-term change in the central Sierra Nevada, California, *J. Geophys. Res.*, *112*, D11124, doi:10.1029/2006JD007561.

Lundquist, J. D., N. C. Pepin, and C. Rochford (2008), Automated algorithm for mapping regions of cold-air pooling in complex terrain, *J. Geophys. Res.*, *113*, D22107, doi:10.1029/2008JD009879.

Maki, M., and T. Harimaya (1988), The effect of advection and accumulation of downslope cold air on nocturnal cooling in basins, *J. Meteorol. Soc. Jpn.*, *66*, 581–597.

Mantua, N. J., S. R. Hare, Y. Zhang, J. M. Wallace, and R. C. Francis (1997), A Pacific interdecadal climate oscillation with impacts on salmon production, *Bull. Am. Meteorol. Soc.*, *78*, 1069–1079, doi:10.1175/1520-0477(1997)078<1069:APICOW>2.0.CO;2.

Mearns, L. O., et al. (2001), Climate scenario development, in *Climate Change 2001: The Science of Climate Change*, edited by J. T. Houghton et al., chap. 13, pp. 739–768, Cambridge Univ. Press, Cambridge, U. K.

Menne, M. J., C. N. Williams, and R. S. Vose (2009), The United States Historical Climatology Network monthly temperature data, version 2, *Bull. Am. Meteorol. Soc.*, *90*, 993–1007, doi:10.1175/2008BAMS2613.1.

Millar, C. I., and R. D. Westfall (2007), Sierra Nevada rock glaciers: Biodiversity refugia in a warming world?, *Eos Trans. AGU*, *88*(52), Fall Meet. Suppl., Abstract GC41A-0098.

Mote, P. W., A. F. Hamlet, M. P. Clark, and D. P. Lettenmaier (2005), Declining mountain snowpack in western north America, *Bull. Am. Meteorol. Soc.*, *86*, 39–49, doi:10.1175/BAMS-86-1-39.

Murphy, J. (2000), Predictions of climate change over Europe using statistical and dynamical downscaling techniques, *Int. J. Climatol.*, *20*(5),

489–501, doi:10.1002/(SICI)1097-0088(200004)20:5<489::AID-JOC484>3.0.CO;2-6.
Neff, W. D., and C. W. King (1989), The accumulation and pooling of drainage flows in a large basin, *J. Appl. Meteorol.*, *28*, 518–529, doi:10.1175/1520-0450(1989)028<0518:TAAPOD>2.0.CO;2.
Oerlemans, J. (2001), *Glaciers and Climate Change*, 160 pp., A. A. Balkema, Lisse, Netherlands.
Pagès, M., J. R. Miró, and A. Sairouni (2008), Determining temperature lapse rates over mountain slopes using modified GWR in the Pyrenees area, 13th Conference on Mountain Meteorology, Am. Meteorol. Soc., Whistler, B. C., Canada.
Pepin, N. C. (2001), Lapse rate changes in northern England, *Theor. Appl. Climatol.*, *68*(1/2), 1–16.
Pepin, N. C., and M. Losleben (2002), Climate change in the Colorado Rocky Mountains: Free-air versus surface temperature trends, *Int. J. Climatol.*, *22*, 311–329, doi:10.1002/joc.740.
Pepin, N. C., and J. D. Lundquist (2008), Temperature trends at high elevations: Patterns across the globe, *Geophys. Res. Lett.*, *35*, L14701, doi:10.1029/2008GL034026.
Pepin, N. C., and D. J. Seidel (2005), A global comparison of surface and free-air temperatures at high elevations, *J. Geophys. Res.*, *110*, D03104, doi:10.1029/2004JD005047.
Peterson, T. C., and R. S. Vose (1997), An overview of the Global Historical Climatology Network temperature database, *Bull. Am. Meteorol. Soc.*, *78*, 2837–2849, doi:10.1175/1520-0477(1997)078<2837:AOOTGH>2.0.CO;2.
Pinto, J. G., U. Ulbrich, G. C. Leckebusch, T. Spangehl, M. Reyers, and S. Zacharias (2007), Changes in storm track and cyclone activity in three SRES ensemble experiments with the ECHAM5/MPI-OM1 GCM, *Clim. Dyn.*, *29*, 195–210, doi:10.1007/s00382-007-0230-4.
Pypker, T. G., M. H. Unsworth, A. C. Mix, W. Rugh, T. Ocheltree, K. Alstad, and B. J. Bond (2007), Using nocturnal cold-air drainage flow to monitor ecosystem processes in complex terrain, *Ecol. Appl.*, *17*(3), 702–714, doi:10.1890/05-1906.
Sairouni, A., J. Moré, J. Toda, J. R. Miró, M. Aran, and J. Cunillera (2008), *Operative Mesoscale Models Verification Running in the Meteorological Service of Catalonia* [in Catalan], *Notes Estudi Serv. Meteorol. Catalunya*, vol. 71, Serv. Meteorol. de Catalunya, Barcelona, Spain.
Santer, B. D., T. M. L. Wigley, J. S. Boyle, D. J. Gaffen, J. J. Hnilo, D. Nychka, D. E. Parker, and K. E. Taylor (2000), Statistical significance of trends and trend differences in layer-average atmospheric time series, *J. Geophys. Res.*, *105*, 7337–7356, doi:10.1029/1999JD901105.
Sheridan, P., S. Smith, A. Brown, and S. Vosper (2010), A simple height-based correction for temperature downscaling in complex terrain, *Meteorol. Appl.*, *17*, 329–339.
Smith, R., et al. (1997), Local and remote effects of mountains on weather: Research needs and opportunities, *Bull. Am. Meteorol. Soc.*, *78*, 877–892.
Solomon, S., D. Qin, M. Manning, Z. Chen, M. Marquis, K. B. Averyt, M. Tignor, and H. L. Miller (Eds.) (2007), *Climate Change 2007: The Physical Science Basis—Contribution of Working Group 1 to the Fourth Assessment Report of the Intergovernmental Panel on Climate Change*, 996 pp., Cambridge Univ. Press, Cambridge, U. K.
Stahl, K., R. D. Moore, J. A. Floyer, M. G. Asplin, and I. G. McKendry (2006), Comparison of approaches for spatial interpolation of daily air temperature in a large region with complex topography and highly variable station density, *Agric. For. Meteorol.*, *139*, 224–236, doi:10.1016/j.agrformet.2006.07.004.
Stewart, J. R., and A. M. Lister (2001), Cryptic northern refugia and the origins of the modern biota, *Trends Ecol. Evol.*, *16*, 608–613, doi:10.1016/S0169-5347(01)02338-2.
Stoermer, E. F., and J. P. Smol (2001), *The Diatoms: Applications for the Environmental and Earth Sciences*, 482 pp., Cambridge Univ. Press, Cambridge, U. K.
Tenow, O., and A. Nilssen (1990), Egg cold hardiness and topoclimatic limitations to outbreaks of *Epirrita autumnata* in northern Fennoscandia, *J. Appl. Ecol.*, *27*, 723–734, doi:10.2307/2404314.
Ulbrich, U. (2009), Extra-tropical cyclones in the present and future climate: A review, *Theor. Appl. Climatol.*, *96*(1–2), 117–131, doi:10.1007/s00704-008-0083-8.
Virtanen, T., S. Neuvonen, and A. Nikula (1998), Modelling topoclimatic patterns of egg mortality of *Epirrita autumnata* (Lepidoptera: Geometridae) with a Geographical Information System: Predictions for current climate and warmer climate scenarios, *J. Appl. Ecol.*, *35*, 311–322, doi:10.1046/j.1365-2664.1998.00299.x.
Vuille, M., R. S. Bradley, M. Werner, and F. Keimig (2003), 20th century climate change in the tropical Andes: Observations and model results, *Clim. Change*, *59*, 75–99, doi:10.1023/A:1024406427519.
Whiteman, C. D. (1982), Breakup of temperature inversions in deep mountain valleys: Part I. Observations, *J. Appl. Meteorol.*, *21*, 270–289, doi:10.1175/1520-0450(1982)021<0270:BOTIID>2.0.CO;2.
Whiteman, C. D., X. Bian, and S. Zhong (1999), Wintertime evolution of the temperature inversion in the Colorado Plateau basin, *J. Appl. Meteorol.*, *38*, 1103–1117, doi:10.1175/1520-0450(1999)038<1103:WEOTTI>2.0.CO;2.
Whiteman, C. D., B. Pospichal, S. Eisenbach, P. Weihs, C. B. Clements, R. Steinacker, E. Mursch-Radlgruber, and M. Dorninger (2004a), Inversion breakup in small Rocky Mountain and Alpine basins, *J. Appl. Meteorol.*, *43*, 1069–1082, doi:10.1175/1520-0450(2004)043<1069:IBISRM>2.0.CO;2.
Whiteman, C. D., T. Haiden, B. Pospichal, S. Eisenbach, and R. Steinacker (2004b), Minimum temperatures, diurnal temperature ranges, and temperature inversions in limestone sinkholes of different sizes, and shape, *J. Appl. Meteorol.*, *43*, 1224–1236, doi:10.1175/1520-0450(2004)043<1224:MTDTRA>2.0.CO;2.
Wilby, R. L., and T. M. L. Wigley (1997), Downscaling general circulation model output: A review of methods and limitations, *Prog. Phys. Geogr.*, *21*, 530–548, doi:10.1177/030913339702100403.
Wilby, R. L., L. E. Hay, and G. H. Leavesley (1999), A comparison of downscaled and raw GCM output: Implications for climate change scenarios in the San Juan River basin, Colorado, *J. Hydrol.*, *225*(1–2), 67–91, doi:10.1016/S0022-1694(99)00136-5.
Yarnal, B. (1993), *Synoptic Climatology in Environmental Analysis*, 195 pp., Belhaven, London.
Yin, J. H. (2005), A consistent poleward shift of the storm tracks in simulations of 21st century climate, *Geophys. Res. Lett.*, *32*, L18701, doi:10.1029/2005GL023684.
Yoshino, M. M. (1975), *Climate in a Small Area*, 549 pp., Univ. of Tokyo Press, Tokyo.
Yoshino, M. M. (1984), Thermal belt and cold air drainage on the mountain slope and cold air lake in the basin at quiet, clear night, *GeoJournal*, *8*, 235–250, doi:10.1007/BF00446473.
You, Q. L., S. C. Kang, N. C. Pepin, and Y. P. Yan (2008), Relationship between trends in temperature extremes and elevation in the eastern and central Tibetan Plateau, 1961–2005, *Geophys. Res. Lett.*, *35*, L04704, doi:10.1029/2007GL032669.

C. Daly, Department of Geosciences, Oregon State University, Corvallis, OR 97331, USA. (chris.daly@oregonstate.edu)
J. Lundquist, Department of Civil and Environmental Engineering, University of Washington, Seattle, WA 98195, USA. (jdlund@u.washington.edu)
N. C. Pepin, Department of Geography, University of Portsmouth, Portsmouth PO1 3HE, UK. (nicholas.pepin@port.ac.uk)